Available online at www.sciencedirect.com
ScienceDirect
Journal of Sound and Vibration 321 (2009) 26–44
JOURNAL OF SOUND AND VIBRATION
www.elsevier.com/locate/jsvi

Modelling of tonal noise control from subsonic axial fans using flow control obstructions

Anthony Gérard[a,*], Alain Berry[a], Patrice Masson[a], Yves Gervais[b]

[a]G.A.U.S., Mechanical Engineering Department, Université de Sherbrooke, Sherbrooke, Québec, Canada J1K 2R1
[b]L.E.A., Université de Poitiers, 40 Av. du Recteur Pineau, Bat. K, 86022 Poitiers Cedex, France

Accepted 11 September 2008
The peer review of this article was organised by the Guest Editor
Available online 31 October 2008

Abstract

This paper investigates the analytical calculation of blade unsteady lift spectrum when interacting with a neighboring obstruction, designed to control tonal noise. The approach used in this paper is to add a secondary unsteady lift mode, of equal intensity but opposite in phase with the primary unsteady lift mode which radiates most of tonal noise, so that the resultant of both primary and secondary modes is null. To control one unsteady lift mode (consequently an acoustic tone) without affecting the harmonics of the controlled mode (consequently the harmonics of the acoustic tone to be controlled), it is important for the secondary unsteady lift to be harmonically selective. We have therefore evaluated the harmonic content of the blade unsteady lift generated by the proposed control obstructions. To this purpose, an original equation is derived using the infinitesimal radial strips theory coupled with the one-dimensional Sears gust analysis. The spectrum of the blade unsteady lift is then analyzed for three types of obstructions: a series of B-trapezoidal obstructions, a B-periodic sinusoidal obstruction and a series of B-rectangular obstructions (where B is the number of blades). The use of salient obstructions leads to a large unsteady lift harmonic content. An optimized wake width of the trapezoidal obstruction leads to a low harmonic content rate of 5.5%. A Gaussian approximation of the measured inflow velocity profile generated by a sinusoidal obstruction leads to a relatively low harmonic content rate of 18.8%, which indicates that most of the energy is contained in the fundamental mode of the blade unsteady lift. Finally, a rotor/rectangular interaction shows that the use of small-width rectangular obstructions leads to a higher harmonic content rate of 58.6%.

1. Introduction

In this paper, a passive method is proposed for reducing the forces responsible for the tonal noise from subsonic axial-flow fans using flow obstructions [1]. Tonal noise is mainly generated by the non-uniform flow entering the fan, leading to fluctuating unsteady forces acting by the blades on the fluid. When decomposing these forces using circumferential Fourier transform, it can be seen that few circumferential modes are responsible for the tonal noise, especially for acoustically compact fans. Therefore, it is herein proposed to adequately position a flow control obstruction in order to destructively interfere with the most radiating

*Corresponding author. Tel.: +1 819 821 8000x63161; fax: +1 819 821 7163.
E-mail address: Anthony.Gerard@USherbrooke.ca (A. Gérard).

0022-460X/$ - see front matter © 2008 Elsevier Ltd. All rights reserved.
doi:10.1016/j.jsv.2008.09.027

Nomenclature

a	circumferential Gaussian width parameter
a_R	radial Gaussian width parameter
B	number of blades
c_0	speed of sound, ($\mathrm{m\,s^{-1}}$)
C	chord of the blade (m)
d	width of rectangular obstruction (m)
D	harmonic content rate (%)
F', F''	lift per unit span ($\mathrm{N\,m^{-1}}$) and per unit area ($\mathrm{N\,m^{-2}}$)
i	imaginary number $\sqrt{-1}$
J_n, K_n	ordinary and modified Bessel functions, nth order
k_0	acoustic wavenumber, $k_0 = \omega/c_0$ ($\mathrm{rad\,m^{-1}}$)
k_θ	circumferential wavenumber $k_\theta = w/R$ ($\mathrm{rad\,m^{-1}}$)
$\tilde{L}$	unsteady lift (N)
M_r	rotational Mach number $M_r = \Omega R/c_0$
n	circumferential harmonic order of N, $w = nN$
$n_{\max}$	maximum circumferential harmonic order of N
N	number of rectangular or trapezoidal obstructions, or number of lobes of the sinusoidal obstruction $N = 2\pi/\theta_0$
p	acoustic pressure (Pa)
R	radius (m)
R_1, R_2	inner and outer radius of obstructions (m)
R_m	mean radius $R_m = 0.7 \times R_T$ (m)
R_H, R_T	fan hub and tip radii (m)
S	incompressible Sears function
S_c	compressible Sears function
t	time (s)
U	tangential velocity of the rotor $U(R) = R\Omega$ ($\mathrm{m\,s^{-1}}$)
$v, \tilde{V}$	spatial and spectral transversal inflow velocity ($\mathrm{m\,s^{-1}}$)
v_0	circumferential uniform velocity term ($\mathrm{m\,s^{-1}}$)
v_m	magnitude of the inflow velocity defect ($\mathrm{m\,s^{-1}}$)
w	circumferential order
$w_{\max}$	maximum circumferential order
$\mathbf{x}; r, \varphi, \alpha$	acoustic field point coordinate, spherical coordinates
γ	rotor blade pitch angle (rad)
θ	circumferential angle (rad)
θ_0	angular period (rad)
θ_c	phase variation of the chord along the span (rad)
θ_g	phase variation of the gust along the span (rad)
Θ	angle of the obstruction (rad)
ρ_0	density of air ($\mathrm{kg\,m^{-3}}$)
σ_θ	reduced frequency $\sigma_\theta = k_\theta C/2$
ω	angular frequency ($\mathrm{rad\,s^{-1}}$)
Ω	angular velocity of the rotor ($\mathrm{rad\,s^{-1}}$)

Subscripts

m	acoustic frequency index
p	primary
s	secondary

primary circumferential mode of the fluctuating force. The concept of controlling tonal noise by adding flow control obstructions has been investigated by a few authors [2–5]. The first preliminary theoretical study about the potential of using flow control obstructions to control fan tonal noise was conducted by Nelson [3]. He considered the use of $2N$ independent flow obstructions to control N modes in order to attenuate the fan tonal noise generated by inlet flow distorsions. The amplitude of the wake deficit behind each obstruction is calculated so that it minimizes a weighted sum of the sound power at the blade passage frequency (BPF) and its harmonics. The risk of amplification of the harmonics of the BPF while attempting to control the sound power at BPF was pointed out. The only modelling of the rotor/flow control obstruction was proposed by Polacsek and Desbois-Lavergne [2]. They used a computational aeroacoustic model based on a Reynolds averaged Navier–Stokes two-dimensional solver to estimate the unsteady force components on blades due to the control cylindrical obstructions. The magnitude of several circumferential unsteady force modes is found to be non-negligible so that the control of the BPF tone can increase the harmonics of the BPF. In previous literature about the passive approach described above, there is no investigation on designing obstructions that do not affect the upper harmonics while controlling an acoustic tone. Others [6] proposed several strategies for reduction of turbomachinery fan noise such as the removal of the blade boundary layer and the addition of

fluid through the rotor blade trailing edge to minimize the wakes shed by the rotor blades, thus making the flow in the stator more uniform, reducing unsteady loading and radiated noise. An unsteady, thin shear layer Navier–Stokes calculation on the stator was used to provide a numerical parametrization of the effects of Gaussian wake widths generated by the rotor, and impinging in the stator vanes, on the amplitude of the acoustic mode propagating in the duct. They concluded that a wake width approximatively equal to the rotor pitch leads to maximize the amplitude of the BPF with respect to its higher harmonics. In this paper, by contrast to Ref. [6], the wake is generated by the control obstruction and impinges inthe rotor. A simple integral equation is derived in this paper to predict analytically the spectrum of the rotor blade unsteady lift generated by the flow control obstructions.

The modelling of airfoil or blade unsteady lift is a topic of research since the beginning of the 20th century with the analysis of a flat plate in a sinusoidally oscillatory motion [7]. Sears obtained a fundamental result on the fluctuating lift experienced by an airfoil passing through a transversal sinusoidal gust [8], based on the "airfoil theory for non-uniform motion" [9]. Afterwards, models have been further investigated to take two-dimensional gusts [10–12] and compressibility effect [13] into account. More recently, the Sears problem has been revisited to include the effect of mean flow angle of attack and the airfoil camber on the gust response [14] and more sophisticated methods to assess the importance of nonlinearity have been presented. An analysis on the three-dimensional effects of blade force on the sound generated by an annular cascade in distorted flows has also been investigated [16], which is particularly adapted for subsonic ducted-fans. Finally, in the last decade, several numerical studies attempted to calculate the unsteady blade forces with the objective to predict tonal noise [17–20]. The numerical approach has been discarded in this study, and instead a simpler and faster analytical method based on the compressible approximation of the Sears function derived by Amiet [13] is used. A periodic inflow distortion due to the interaction of rotating blades with a neighboring obstruction is either imposed or fitted from experimental measurements. This inflow velocity serves as an input for the calculation of the unsteady lift per unit span at a given radius. The unsteady lift is then calculated by integrating the unsteady lift per unit span along the span using an infinitesimal strip theory, which can be done by assuming that the problem can be locally treated as a one-dimensional problem. The sweep of the blades and the phase of the gust along the span are taken into account. The calculation is performed into the spectral domain since the periodic unsteady lift responsible for tonal noise is of interest. The final objective is to evaluate the unsteady lift spectra generated by the interaction between the rotor and the control obstructions and to choose the obstruction leading to the lowest harmonic content of the blade unsteady lift. From a control point of view, the ideal case would be a pure sinusoidal flow field pattern, leading to a single circumferential unsteady lift mode. In such a case, it is possible to control each unsteady lift mode independently, and thus control an acoustic tone without affecting the other tones.

In this paper, the control approach is first conceptually described. Then, the Sears theory associated to the infinitesimal strip theory is reviewed to calculate the unsteady lift generated by the interaction between a rotor and an obstruction. Finally, numerical examples are given for various obstruction types (trapezoidal, sinusoidal and rectangular obstructions). An optimization of the wake width generated by the trapezoidal obstruction is also investigated. Circumferential wavenumber spectra of the blade unsteady lift produced by the interaction between the rotor and the control obstructions are presented and a harmonic content analysis is carried out to evaluate the ability of the control obstructions to selectively control a blade unsteady lift mode.

2. Control approach

2.1. Tonal noise from subsonic fans

The rotor is considered as an array of rotating surfaces. When the fan tip Mach number is subsonic, as is the case for automotive engine cooling fans investigated in this paper, the monopolar thickness noise and the turbulent quadripolar terms can be neglected [23]. In order to examine the acoustic radiation of axial fans, it is convenient to use the polar coordinate system (R, θ, y_3) to describe the sources on the blades and the spherical coordinate system (r, φ, α) to describe the acoustic free field, as shown in Fig. 1. Both coordinate system origins are located at the center of the rotor. Following Blake [23], the lift per unit span on the blades $F'(R, t)$ is

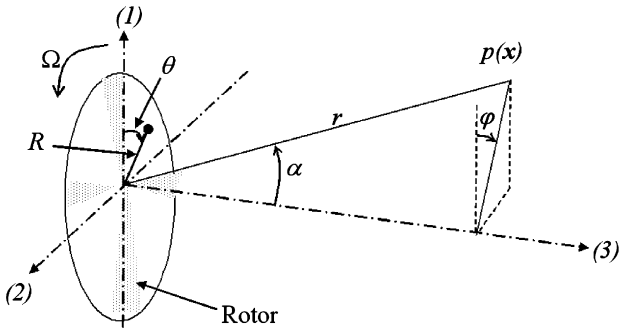

Fig. 1. Sound radiation from a fan (coordinate systems).

calculated by integrating the instantaneous pressure differential across the rotor $F''(R,\theta_b,t)$ along the chord $(-C/2R<\theta_b<C/2R)$. The forces are considered to be concentrated in the plane of the rotor at $y_3=0$. For a circumferentially periodic inflow disturbance composed of wavelengths $2\pi R/w$ (where $w=]-\infty;+\infty[$ is the Fourier circumferential harmonic order of the disturbance), the circumferential and radial distribution of the fluctuating lift on the rotor blades in a frame rotating with the rotor can be expressed as follows:

$$\frac{\mathrm{d}L(R,\theta,t)}{\mathrm{d}R}=\sum_{b=0}^{B-1}\sum_{w=-\infty}^{w=+\infty}\frac{\mathrm{d}\tilde{L}(w,R)}{\mathrm{d}R}\mathrm{e}^{-\mathrm{i}w\Omega t}\mathrm{e}^{\mathrm{i}w\theta}\delta\left(\theta-b\frac{2\pi}{B}\right) \tag{1}$$

where the index b refers to the blades and the index w refers to the circumferential harmonic order of the lift, B is the number of blades and Ω is the rotation speed of the rotor in rad s^{-1}. Eq. (1) represents a series of B line forces spaced at regular intervals $2\pi/B$ around the circumferential direction. As opposed to what was presented by Blake [23], the phase of the lift along the span (due to the sweep of the blade or the incident gust) is taken into account in the circumferential harmonic decomposition of the unsteady lift per unit span $\mathrm{d}\tilde{L}(w,R)/\mathrm{d}R$. Then, Blake obtained the sound pressure $p(\mathbf{x},t)$, radiated by B blades at location $\mathbf{x}=(r,\varphi,\alpha)$ (see Fig. 1), by integrating (over the span) the product of the lift per unit span $\mathrm{d}\tilde{L}(w,R)/\mathrm{d}R$, projected over circumferential mode w and the appropriate Green function for rotating dipolar sources in free field. The far-field approximation ($r\gg R$) is given by

$$p(\mathbf{x},t)=\sum_{m=-\infty}^{\infty}\sum_{w=-\infty}^{\infty}[P(\mathbf{x},\omega)]_{w,m}\mathrm{e}^{-\mathrm{i}mB\Omega t} \tag{2}$$

with

$$[P(\mathbf{x},\omega)]_{w,m}=\underbrace{\frac{-\mathrm{i}k_0B\mathrm{e}^{\mathrm{i}k_0r}}{4\pi r}\mathrm{e}^{-\mathrm{i}(mB-w)(\pi/2-\varphi)}\delta(\omega-mB\Omega)}_{\text{Acoustic wave propagation}}\times\int_{R_H}^{R_T}\underbrace{J_{mB-w}(k_0R\sin\alpha)}_{\text{Bessel function term}}$$
$$\times\underbrace{\frac{\mathrm{d}\tilde{L}(w,R)}{\mathrm{d}R}}_{\text{Unsteady lift per unit span}}\times\left[\underbrace{\cos\gamma\cos\alpha}_{\substack{\text{Axial forces}\\ \text{contribution}}}+\underbrace{\frac{mB-w}{k_0R}\sin\gamma}_{\substack{\text{Tangential forces}\\ \text{contribution}}}\right]\mathrm{d}R \tag{3}$$

The first summation of Eq. (2) represents the combination of multiple tones at angular frequencies $\omega=mB\Omega$. The second summation represents the decomposition of the lift over circumferential harmonics w. In Eq. (3), the first term describes the propagation of the acoustic waves, which have a wavenumber $k_0=\omega/c_0$ (where c_0 is the speed of sound) and rotate at a circumferential phase velocity equal to $mB/(mB-w)\Omega$. In the integration over the radius (from the hub radius R_H to tip radius R_T), the Bessel function term refers to the ability of a circumferential mode w to radiate sound at the harmonic of rank m of the BPF $B\Omega$. The term $\mathrm{d}\tilde{L}(w,R)/\mathrm{d}R$ is the contribution of the circumferential mode w to the lift per unit span acting at a radius R.

The terms in brackets weight the relative importance of axial and tangential forces, which are function of the pitch angle γ.

If the spatial extent of the fluctuating pressures on the rotor surface is less than a wavelength of the sound generated, the fan effective area can be reduced to an approximate equivalent distribution of dipoles distributed along a mean radius of the fan $R_m = 0.7 \times R_T$ [23,25]. It is important to keep the unsteady lift per unit span into the integral to take the sweep of the blade and the sweep of the gust into account along the span. Considering the above simplifications, Eq. (3) can be written as

$$[P(\mathbf{x},\omega)]_{w,m} \approx \frac{-\mathrm{i}k_0 B \mathrm{e}^{\mathrm{i}k_0 r}}{4\pi r} \mathrm{e}^{-\mathrm{i}(mB-w)(\pi/2-\varphi)} \delta(\omega - mB\Omega) \times J_{mB-w}(k_0 R_m \sin\alpha) \times \tilde{L}(w) \times \left[\cos\gamma\cos\alpha + \frac{mB-w}{k_0 R_m}\sin\gamma\right] \tag{4}$$

where $\tilde{L}(w)$ is the lift per unit span integrated along the span:

$$\tilde{L}(w) = \int_{R_H}^{R_T} \frac{\mathrm{d}\tilde{L}(w,R)}{\mathrm{d}R}\,\mathrm{d}R \tag{5}$$

Note that the approximate equation (4) is exact and equivalent to Eq. (3) on the fan axis ($\alpha = 0$).

2.2. Principle of the passive adaptive control of tonal noise

From the Bessel function $J_{mB-w}(k_0 R \sin\alpha)$ in Eqs. (3) and (4), it can be seen that the lift circumferential harmonic of order $w = mB$ is the major contributor to the tonal noise at the frequency $mB\Omega$. Thus, controlling this particular mode can lead to large tonal noise reduction in the whole space. In practice, coincidence between w and mB is avoided by choosing a number of stator vanes different to the number of rotor blades for example. However, one can use this coincidence to control the tonal noise at frequency $mB\Omega$ by superimposing a secondary unsteady lift $\tilde{L}_s(w = mB)$ of equal intensity but opposite in phase relative to the most radiating circumferential component $\tilde{L}_p(w = mB)$ of the primary lift, as shown schematically in Fig. 2. Assuming that the primary and secondary inflow velocity field (thus the unsteady lift) can be linearly added, the total sound field $p_t(\mathbf{x},t)$ is the sum of the primary sound field $p_p(\mathbf{x},t)$ and the secondary sound field $p_s(\mathbf{x},t)$:

$$\begin{aligned} p_t(\mathbf{x},t) &= p_p(\mathbf{x},t) + p_s(\mathbf{x},t) \\ &= \sum_{m=-\infty}^{\infty}\sum_{w=-\infty}^{\infty} ([P_p(\mathbf{x},\omega)]_{w,m} + [P_s(\mathbf{x},\omega)]_{w,m})\mathrm{e}^{-\mathrm{i}mB\Omega t} \end{aligned} \tag{6}$$

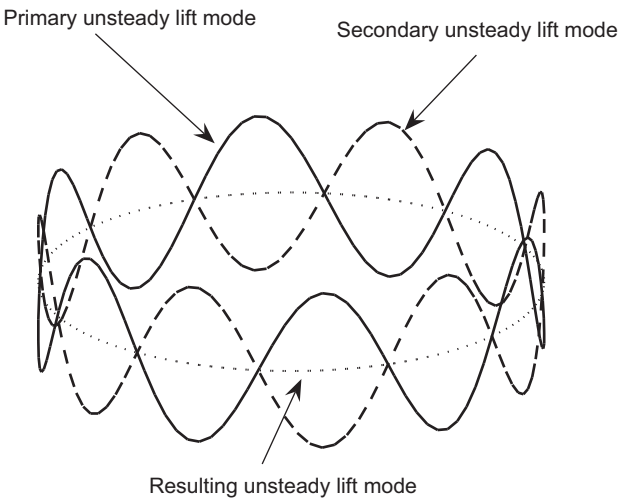

Fig. 2. Principle of the wake generator to control the primary unsteady lift modes.

The linear assumption is verified experimentally in Ref. [1] for the automotive fan under investigation. From Eqs. (2) and (4), the total sound field can be written as a function of the sum of the primary unsteady $\tilde{L}_p(w)$ lift and the secondary unsteady lift $\tilde{L}_s(w)$:

$$p_t(\mathbf{x},t)=\sum_{m=-\infty}^{\infty}\sum_{w=-\infty}^{\infty}[H]_{w,m}(\tilde{L}_p(w)+\tilde{L}_s(w))\mathrm{e}^{-\mathrm{i}mB\Omega t} \tag{7}$$

where $\tilde{L}_s(w=mB)=-\tilde{L}_p(w=mB)$, to control the acoustic radiation at frequency $mB\Omega$ and H is defined as follows:

$$[H]_{w,m}=\frac{-\mathrm{i}k_0B\mathrm{e}^{\mathrm{i}k_0r}}{4\pi r}\mathrm{e}^{-\mathrm{i}(mB-w)(\pi/2-\varphi)}\delta(\omega-mB\Omega)J_{mB-w}(k_0R_m\sin\alpha)\times\left[\cos\gamma\cos\alpha+\frac{mB-w}{k_0R_m}\sin\gamma\right] \tag{8}$$

A solution to reduce the tonal noise from axial fans is thus to create the secondary interaction mode to create a secondary non-uniform flow interacting with the rotor. This secondary non-uniform flow creates a secondary unsteady lift radiating a secondary tonal noise opposite in phase with the primary tonal noise so that the resulting sound is reduced. This can be done using adequately positioned flow control obstruction(s) (also called wake generators by Polacsek et al. [2]). Thus, the control is passive but the position of the obstruction must be adapted to adjust the magnitude and the phase of the secondary interaction mode in order to minimize the tonal acoustic radiation. The adjustment of the distance between the control obstruction and the rotor allows the secondary interaction mode magnitude to be adjusted while the adjustment of the angle of the control obstruction allows the secondary interaction mode phase to be adjusted.

The flow control obstruction must be designed with care to generate the desired secondary unsteady lift mode. Especially, it is important that the obstruction be selective to mainly generate one unsteady lift mode, because other induced lift modes can give rise to sound radiation at higher frequencies. For example, the use of sharp control obstruction(s), such as small diameter cylinders, as proposed in Refs. [2,5,31,32], leads to sharp wakes and thus to a large spectral energetic content of the unsteady lift. The following sections of this paper analyze the circumferential lift spectrum of various proposed control obstructions. The design of a control obstruction geometry which is as spectrally selective as possible is the ultimate goal of the analysis.

3. Unsteady lift generated by control obstructions

This section aims at calculating the unsteady lift $\tilde{L}(w)$ of Eq. (4) generated by various control obstruction geometries. The results will be used to optimize the shape of the obstruction so that its circumferential spectrum of the unsteady lift is selective. Before further investigating the modelling of the flow control obstructions/rotor interaction, the unsteady airfoil theory is summarized. When an airfoil (or a blade) moves into a non-uniform flow, the angle of incidence of the airfoil relative to the airflow is time varying, leading to dynamic pressure distribution fluctuations.

Sears [8] has developed a linear theory for a flat plate of infinitesimal thickness encountering a gust in incompressible flow. The formulation proposed by Sears relates the unsteady lift per unit span to the incident downwash amplitude of the gust. Amiet [13] later on proposed a model for compressible flows. The compressibility effects must be taken into account when the time for an acoustic wave to travel across the blade chord is not negligible compared to the time for a fluid disturbance to cross the blade, which is the case at high frequency. Once the blade unsteady lift per unit span is known along the span, the unsteady lift can be calculated using the strip theory by integrating the unsteady lift per unit span along the span. The sweep of the blades and the sweep of the gust along the blade span must be taken into account.

Based on the classical unsteady airfoil theory and the strip theory, a new simple integral equation is obtained to calculate the rotor unsteady lift generated by the interaction between the rotor and the obstructions, assuming that a Gaussian non-uniform inflow velocity is induced by the obstructions. The variables of this formulation are related to the geometrical characteristics of the rotor and the obstructions, and the characteristic of the non-uniform inflow velocity.

3.1. The Sears function for a transversal gust

Let us consider a one-dimensional periodic gust with transversal velocity $v(\theta,t)$ moving in the circumferential θ-direction at speed U, as illustrated in Fig. 3. The lift response per unit span acting at the quarter-chord point to a transverse gust is given by the expression [23]:

$$\frac{\mathrm{d}\tilde{L}(w,R)}{\mathrm{d}R} = \pi\rho_0 C\tilde{V}(w,R)U(R)S(\sigma_\theta) \tag{9}$$

where ρ_0 is the density of air, C is the blade chord, $U(R)=R\Omega$, is the tangential speed of the rotor at radius R, $\sigma_\theta = k_\theta C/2 = wC/2R$, is the reduced frequency and w is the circumferential order of the gust (number of gust periods per circumference). Also, $\tilde{V}(w,R)$ is the circumferential harmonic decomposition of the inflow velocity normal to the blade chord, such that

$$\tilde{V}(w,R) = \frac{1}{2\pi}\int_0^{2\pi} v(\theta,R)\mathrm{e}^{-\mathrm{i}w\theta}\,\mathrm{d}\theta \tag{10a}$$

and

$$v(\theta,R) = \sum_{w=-\infty}^{\infty} \tilde{V}(w,R)\mathrm{e}^{\mathrm{i}w\theta} \tag{10b}$$

Moreover, in Eq. (9), $S(\sigma_\theta)$ is the incompressible Sears function defined as follows [25]:

$$S(\sigma_\theta) = \frac{1}{\mathrm{i}\sigma_\theta[K_0(\mathrm{i}\sigma_\theta)+K_1(\mathrm{i}\sigma_\theta)]} \tag{11}$$

where K_0 and K_1 are, respectively, the zeroth-order and first-order modified Bessel functions.

To account for the effect of blade camber, thickness and angle of attack of the blade, a second-order analysis must be carried out [22]. However, in order to get explicit mathematical expression of the unsteady lift and simplify the calculation of the unsteady lift spectra generated by the ingestion of control obstruction wakes by the rotor, the linear analysis was considered sufficient. On the other hand, the inclusion of compressibility effects does not much complicate the mathematical expression of the Sears function. If the reduced frequency is large enough, such that the time for an acoustic wave to travel the chord is not negligible in comparison to the time for a blade to travel an inflow velocity disturbance, a compressible Sears function is recommended [22]. The low-frequency approximation of the compressible Sears function derived by Amiet [13] is used:

$$S_c(\sigma_\theta,M_r) = \frac{S(\sigma_\theta/\beta_r^2)}{\beta_r}[J_0(M_r^2\sigma_\theta/\beta_r^2)+\mathrm{i}J_1(M_r^2\sigma_\theta/\beta_r^2)]\mathrm{e}^{-\mathrm{i}\sigma_\theta f(M_r)/\beta_r^2} \tag{12}$$

with

$$\beta_r \equiv \sqrt{1-M_r^2}$$

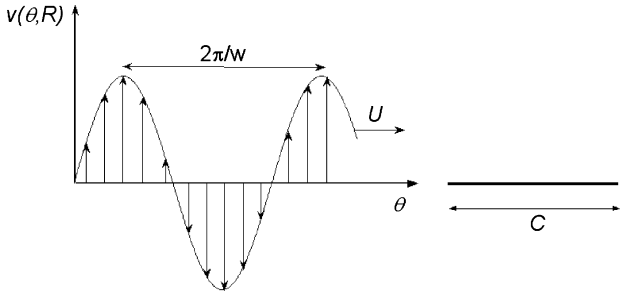

Fig. 3. The Sears problem, blade section submitted to a transversal gust.

and

$$f(M_r) \equiv (1-\beta_r)\ln M_r + \beta_r \ln(1+\beta_r) - \ln 2$$

where $M_r = \Omega R/c_0$, is the rotation Mach number, J_0 and J_1 are, respectively, the zeroth-order and first-order ordinary Bessel functions. A criterion for the applicability of Eq. (12) is given by Amiet [13]: $\sigma_\theta M_r/\beta_r^2 < 1$, or $w < 2R(1-M_r^2)/CM_r$. This condition is satisfied up to the circumferential order $w_{\max} = 43$, for a $C = 5\,\text{cm}$ blade chord, rotating at $\Omega = 2\pi \times 50\,\text{rad}\,\text{s}^{-1}$, at a 10 cm radius. This condition therefore provides an upper bound of the circumferential harmonic w in Eq. (9).

3.2. The infinitesimal strip theory

In this paper, instead of considering an oblique gust impinging the blades (with a radial and a circumferential wavenumber, which is referred to as the two-dimensional gust problem), the fan rotor is decomposed into infinitesimal radial strips along the span, which individually respond to a transversal gust. In other words, at a given radius, the gust and the blade are considered of infinite span so that the gust interaction problem can be treated as a one-dimensional gust problem, as in the previous section. The unsteady lift per unit span (Eq. (9)) is then integrated along the span to yield the unsteady lift on the blade:

$$\begin{aligned}\tilde{L}(w) &= \int_{R_H}^{R_T} \frac{\mathrm{d}\tilde{L}(w,R)}{\mathrm{d}R}\,\mathrm{d}R \\ &= \pi\rho_0\Omega \int_{R_H}^{R_T} C(R)R\tilde{V}(w,R)\mathrm{e}^{\mathrm{i}w(\theta_c(R)-\theta_g(R))}S_c(\sigma_\theta, M_r)\,\mathrm{d}R \end{aligned} \tag{13}$$

where R_H and R_T are, respectively, the hub and tip radii of the rotor. In the problem of upstream obstructions generating circumferential inflow fluctuations, the transversal velocity of the gust $\tilde{V}(w,R)$ is the unknown in Eq. (13). By approximating $v(\theta,R)$ by a Gaussian function of θ behind the obstructions, it is possible to calculate its Fourier transform $\tilde{V}(w,R)$. Since the transversal velocity is decomposed into infinitesimal strips, the phase variation of the gust along the span $\theta_g(R)$ relatively to the phase of the chord along the span $\theta_c(R)$ (due to the sweep of the blade) must be taken into account. In Fig. 4, four blades and four regularly spaced obstructions are chosen to show the coordinate system used to described the sweep of the blades and the gust along the span. A square shape of the obstruction is chosen for illustration purpose.

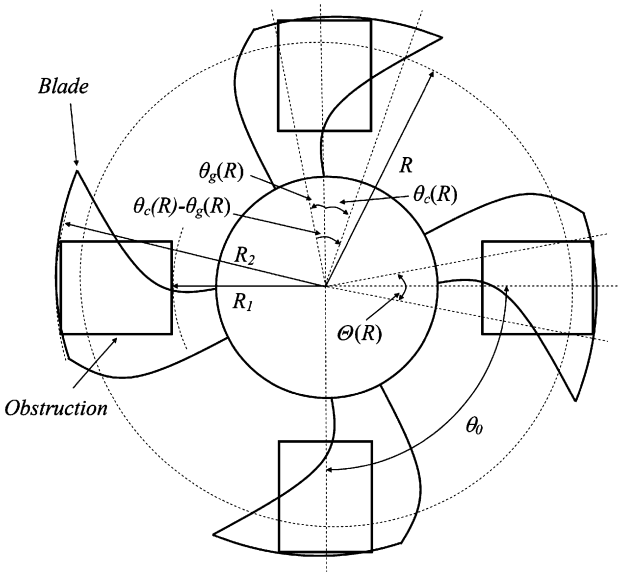

Fig. 4. Problem geometry.

3.2.1. Spatial transversal velocity

Since the flow responsible for tonal noise is non-uniform but stationary, a deterministic periodic spatial transversal velocity $v(\theta, R)$ is imposed over the circumferential direction θ. The flow is considered uniform in the region without obstruction $[R_H, R_1[$ and $]R_2, R_T]$, where R_1 and R_2 are, respectively, the inner and outer radii of the obstructions (cf. Fig. 4). Thus the calculation of Eq. (13) and the spatial Fourier transform $\tilde{V}(w, R)$ of $v(\theta, R)$ is only required in the interval $[R_1, R_2]$. A Gaussian velocity profile is assumed behind the portion occupied by the obstruction. The angular width of the Gaussian profile is related to the angle $\Theta(R)$ of the obstruction at radius R, so that the transversal velocity can be written as follows:

$$v(\theta, R) = v_0(R) + v_m(R) \sum_{n=-\infty}^{+\infty} \mathrm{e}^{-((\theta - n\theta_0)/a(R)\Theta(R))^2}, \quad R_1 \geqslant R \geqslant R_2 \tag{14}$$

where $a(R)$ is the Gaussian width parameter, $v_m(R)$ is the magnitude of the inflow velocity defect and θ_0 is the angular period of the obstruction(s) as defined in Figs. 4 and 5. The uniform velocity term $v_0(R)$ can be ignored in Eq. (14) since it does not contribute to the unsteady lift and sound radiation at low subsonic blade speed. In Eq. (14), rather than considering the superposition of Gaussian inflow velocity only between 0 and 2π (a single cycle), we consider an infinity of Gaussians for an infinity of cycles (like an unrolled rotor $-\infty < \theta < +\infty$). This summation is then useful to simplify the expression of the inflow velocity by using the Poisson formula.

The Gaussian inflow velocity distortion assumption is versatile since the magnitude and the angular width of the Gaussian function can be adjusted as a function of the radius R to account for the distance of the obstruction/rotor axial distance, the rotation speed of the fan, the aerodynamic shape of the obstruction. Published inflow velocity measurements show Gaussian shape of the mean velocity profiles in the downstream flow field of various obstructions in various operating conditions [26–29]. Experimental results reported later in this paper (Section 4.2) also show the ability of a Gaussian function to approximate the measurement of the wake velocity profile generated by a sinusoidal obstruction. However, for a large angular obstruction located very close to the rotor, a flat top velocity profile would be more appropriate.

In order to simplify the calculation of the Fourier transform of the spatial transversal velocity, it is useful to introduce the following variable:

$$A^2(R) = \frac{\theta_0^2}{a^2\Theta(R)^2} = \frac{4\pi^2}{a^2N^2\Theta(R)^2} \tag{15}$$

where N is the number of obstructions regularly spaced over the circumferential direction and where the Gaussian width parameter $a(R)$ is considered independent of the radius R. Making use of the Poisson summation formula: $\sum_{n=-\infty}^{+\infty} f(n) = \sum_{m=-\infty}^{+\infty} \int_{-\infty}^{+\infty} f(z)\mathrm{e}^{-2\pi imz}\,\mathrm{d}z$, with $f(n) = \mathrm{e}^{-((\theta - n\theta_0)/a\Theta(R))^2}$, the transversal

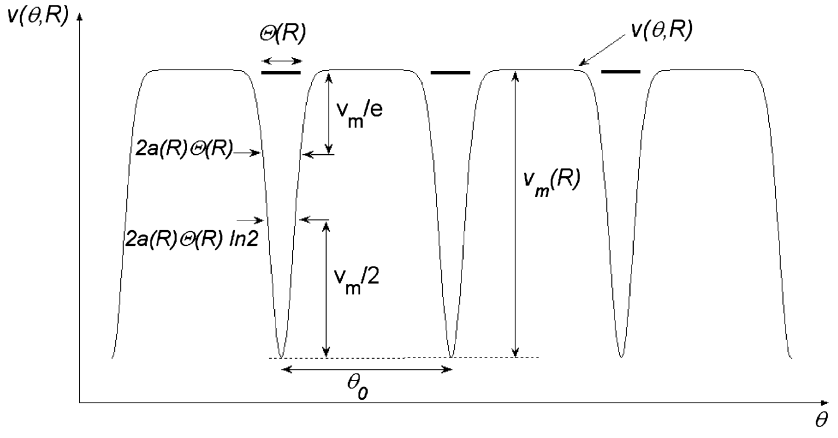

Fig. 5. Gaussian wake velocity defect generated by upstream angular segments of width $\Theta(R)$.

velocity can be rearranged after introducing the variable $\xi = A(\theta/\theta_0 - z)$:

$$\int_{-\infty}^{+\infty} f(z)\mathrm{e}^{-2\mathrm{i}\pi imz}\,\mathrm{d}z = -\frac{1}{A(R)}\mathrm{e}^{-2\mathrm{i}\pi m(\theta/\theta_0)-m^2\pi^2/A^2(R)}\int_{-\infty}^{+\infty}\mathrm{e}^{-(\xi-\mathrm{i}m\pi/A(R))^2}\,\mathrm{d}\xi \tag{16}$$

Since $\int_{-\infty}^{+\infty}\mathrm{e}^{-(\xi-\mathrm{i}m\pi/A)^2}\,\mathrm{d}\xi = \sqrt{\pi}$ [30], the expansion of the spatial transversal velocity over the circumferential direction is

$$v(\theta,R) = -v_m(R)\frac{\sqrt{\pi}}{A(R)}\sum_{m=-\infty}^{+\infty}\mathrm{e}^{-2\mathrm{i}\pi m(\theta/\theta_0)-m^2\pi^2/A^2(R)} \tag{17}$$

The spatial velocity profile behind the obstructions given by Eq. (17) is then Fourier transformed into the circumferential spectral domain and Eq. (13) is used to obtain the unsteady lift of the rotor blades as a function of the circumferential spectral components of the velocity.

3.2.2. Spectral transversal velocity

The Fourier transform $\tilde{V}(w,R)$ of the transversal velocity $v(\theta,R)$ is given by Eq. (10a), where the fundamental circumferential order is equal to the number of obstructions $2\pi/\theta_0 = N$. All circumferential orders appearing in Eq. (10b) will be multiples of N. Calculating the Fourier transform of Eq. (10a) over only one angular period θ_0 leads to the following expression of the spatial Fourier transform of the transversal velocity:

$$\tilde{V}(nN,R) = -\frac{v_m(R)\sqrt{\pi}}{A(R)}\sum_{m=-\infty}^{+\infty}\mathrm{sinc}(\pi(m+n))\mathrm{e}^{-m^2\pi^2/A^2(R)} \tag{18}$$

3.3. Unsteady lift integrated along the span

Eq. (18) is introduced into Eq. (13) with $R_H = R_1$, and $R_T = R_2$, to give the general expression of the unsteady lift for the circumferential order $w = nN$, caused by N regularly spaced obstructions generating Gaussian wakes:

$$\tilde{L}(nN) = \pi^{3/2}\rho_0\Omega\sum_{m=-\infty}^{+\infty}\mathrm{sinc}(\pi(m+n))\int_{R_1}^{R_2}\frac{v_m(R)}{A(R)}C(R)Re^{-m^2\pi^2/A^2(R)}\mathrm{e}^{\mathrm{i}w(\theta_c(R)-\theta_g(R))}S_c(\sigma_\theta,M_r)\,\mathrm{d}R \tag{19}$$

where the phase of the gust relative to the blade over the span is taken into account in the term $\mathrm{e}^{\mathrm{i}nN(\theta_c(R)-\theta_g(R))}$. From Fig. 4, it can be seen that $\theta_c(R)$ depends on the sweep of the blade and that the origin of the angular position is chosen so that $\theta_g(R) = \Theta(R)/2$. Introducing Eq. (19) into Eq. (4) leads to the sound pressure field generated by the interaction between the rotor and the flow control obstruction. At the best of the author knowledge, the integral equation (19) is new.

The calculation steps from the spatial velocity profile to the unsteady lift generated by the control obstructions are illustrated in Fig. 6. To illustrate the calculation steps, the inflow velocity was measured at six radii (with hot wire anemometer) behind a sinusoidal obstruction. The velocity shown in Fig. 6a is an adjusted Gaussian approximation of the wake measurement over the circumference and the wake measurements were interpolated over the radius. The spatial velocity profile is then decomposed into strips and Fourier transformed. Fig. 6b shows the circumferential Fourier transform of the spatial velocity as a function of R and w, which serves as input data in Eq. (13). In Fig. 6b, the circumferential Fourier components of the velocity $\tilde{V}(w,R) = 0$, if $w \neq 6n$. This second step is already taken into account in Eq. (19). Finally, the unsteady lift spectrum (Fig. 6c) is obtained by solving the integral of Eq. (19) using the trapezoidal rule (128 radial elements are considered). The infinite sum over m is truncated from $m = -50$ to 50, which has been verified to ensure convergence.

The magnitude of the Gaussian velocity profile $v_m(R)$ influences the unsteady lift magnitude (Eq. (19)) and the magnitude of the radiated tones (via Eq. (4) for acoustically compact blades). For the prediction of the radiated tone magnitude, $v_m(R)$ can be determined experimentally. Nevertheless, the relative magnitudes of the unsteady lift spectral components are sufficient to characterize the shape of the unsteady lift spectrum. Thus,

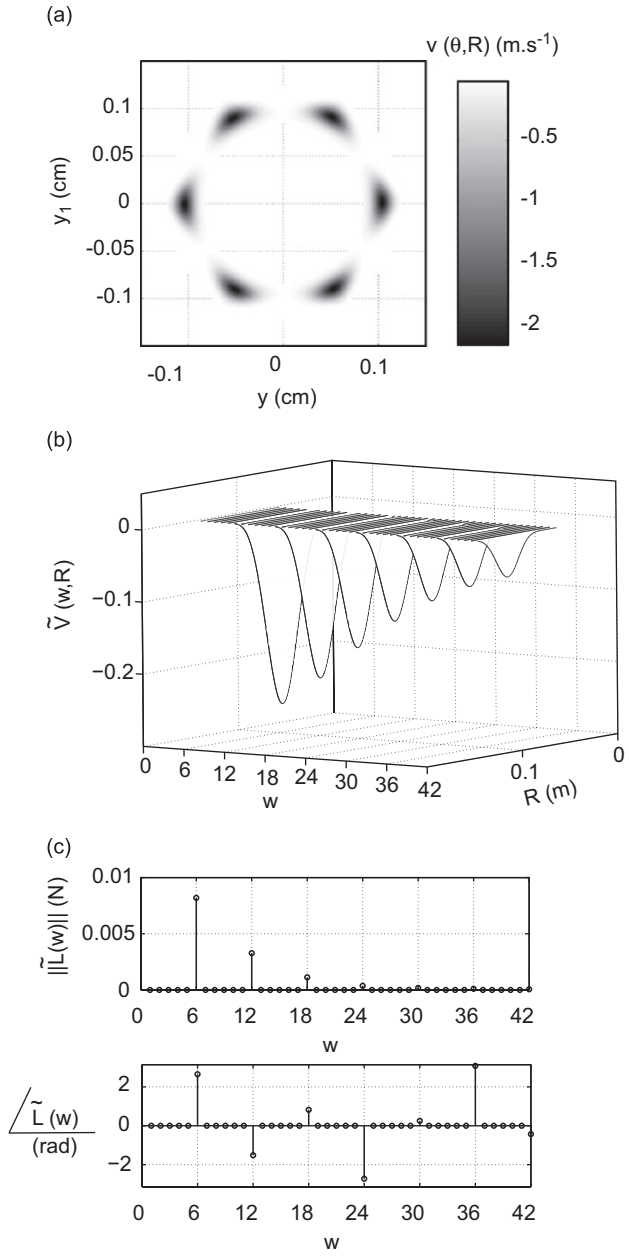

Fig. 6. Illustration of the calculation steps from the spatial velocity profile to the unsteady lift spectrum: (a) spatial velocity profile, (b) spectral velocity profile, (c) unsteady lift spectrum.

as long as the inflow velocity can be approximated by a Gaussian profile, $v_m(R)$ can be imposed arbitrarily. In the following section, the magnitude of the unsteady lift spectral components $\tilde{L}(nN)$ $(n \geqslant 1)$ is normalized to the magnitude of the first component of the unsteady lift spectrum $\tilde{L}(N)$ in order to qualitatively compare the spectra generated by various Gaussian widths of the velocity profile.

4. Numerical examples

Since the experimental investigation has been carried out in this paper for a 6-bladed automotive engine cooling fan with equal blade pitches, regularly spaced obstructions along the circumference are proposed.

The inner and outer radii of the rotor are, respectively, $R_H = 6.25\,\text{cm}$ and $R_T = 15\,\text{cm}$. In the following examples, the control obstruction is designed to control the BPF tone. Three types of obstructions are considered here: a series of $N = 6$ trapezoidal obstructions (Fig. 7a), a continuous $N = 6$-periods sinusoidal obstruction (Fig. 7b) and a series of $N = 6$ rectangular obstructions (Fig. 7c). The three-dimensional shape of the cylinders is not included in the model, i.e. the imposed Gaussian velocity behind cylindrical obstructions of diameter d would be the same as the Gaussian velocity imposed behind rectangular obstructions of width d. The angles $\Theta(R)$ (Fig. 4) of the obstructions at radius R are defined as follows:

$$\Theta(R) = \Theta = \text{Const.}, \quad R_1 \leqslant R \leqslant R_2 \quad \text{Trapezoidal obstructions} \tag{20}$$

$$\Theta(R) = 2\sin^{-1}\frac{d}{2R}, \quad R_1 \leqslant R \leqslant R_2 \quad \text{Cylindrical or rectangular obstructions} \tag{21}$$

$$\Theta(R) = \frac{2}{N}\cos^{-1}\left(\frac{2R - R_1 - R_2}{R_2 - R_1}\right), \quad R_1 \leqslant R \leqslant R_2 \quad \text{Sinusoidal obstruction} \tag{22}$$

In the simulations presented here, the inner and outer radii of the obstructions are, respectively, $R_1 = 8$ and $R_2 = 12\,\text{cm}$. The values of $\Theta(R)$ in Eqs. (20)–(22) have to be introduced into Eq. (15) for the different obstructions under investigation and the Gaussian width parameter a has to be arbitrarily imposed or fitted from inflow velocity measurements in Eq. (15).

The circumferential component $w = B$, of the primary unsteady lift is the most radiating at the BPF, as discussed in Section 2. By adding the obstructions described in this section, a secondary flow is added. Attenuation of the BPF tone is obtained when the circumferential component of the secondary lift $w = N$, is equal and opposite in phase to the circumferential component of the primary lift $w = N$. However, the higher-order circumferential components of the secondary lift $w = nN$ ($n \geqslant 2$), should be as small as possible in order to leave higher harmonics of the BPF unaffected by the control obstruction. Thus, the spectral content of the unsteady lift generated by the control obstructions is of interest. In this respect, the harmonic content rate D (%) is proposed and defined by

$$D\ (\%) = \sqrt{\frac{\sum_{n=2}^{n_{\max}} |\tilde{L}(nN)|^2}{\sum_{n=1}^{n_{\max}} |\tilde{L}(nN)|^2}} \times 100 \tag{23}$$

where $n_{\max}$ is related to the maximum circumferential order $w_{\max}$ in Eq. (19) through $n_{\max} = w_{\max}/N$. The limit $n_{\max} \leqslant 7$, ($w_{\max} = n_{\max} \times 6 = 42$), is imposed by the low frequency approximation of the compressible Sears function when a series of $N = 6$ obstructions is considered, as discussed in Section 3.1.

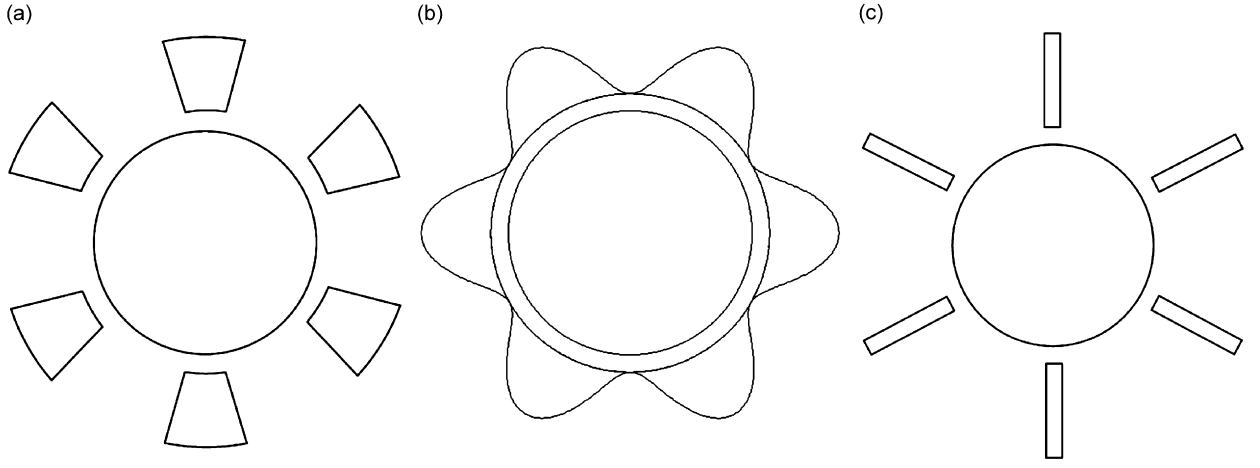

Fig. 7. The obstructions described in this paper: (a) 6-trapezoidal obstructions, (b) 6-periods sinusoidal obstruction, (c) six rectangular obstructions.

Note that an obstruction generating a purely sinusoidal circumferential inflow velocity distribution, thus a purely sinusoidal unsteady lift, would provide the best selection of a given single frequency in the acoustic spectrum of the rotor. In such a case, the harmonic content rate is $D = 0\%$. To control the $m \times BPF$ tone, the number of regularly spaced obstructions must be adjusted such that the fundamental circumferential order of the unsteady lift is $w = N = mB$.

Simulations are first reported for the rotor/trapezoidal obstruction interaction, to show the influence of the product $a\Theta$ and the geometry of the blade on the unsteady lift ($v_m(R)$ is imposed). Then, the unsteady lift generated by the rotor/sinusoidal obstruction interaction is calculated from experimental inflow velocity measurements ($v_m(R)$ is measured). Finally, the unsteady lift generated by the rotor/rectangular obstruction case is considered ($v_m(R)$ is imposed) and compared to the unsteady lift generated by trapezoidal and sinusoidal flow control obstruction. In the following sections, we insist on the qualitative rather than quantitative characterization of the unsteady lift spectra in order to provide a simple analytical tool to help the design of obstructions with low harmonic content rate.

4.1. 6-Trapezoidal obstructions

The case of the 6-trapezoidal obstructions/rotor interaction is useful to study the influence of the Gaussian width parameter a and the angle $\Theta(R) = \Theta = C^{te}$, of the trapezoids. Eq. (15) shows that the parameter of interest is the product $a\Theta$, that is representative of the wake width (Fig. 5). By varying $a\Theta$, it is possible to find out an optimal value of $a\Theta$ so that the harmonic content rate D is minimal, as shown in Fig. 8.

Two blade geometries are considered: 35° trapezoidal blades and the swept blades of an actual automotive fan under investigation in Ref. [1]. For the trapezoidal blades, the minimum of $D = 6.7\%$, and the maximum of the ratio $\|\tilde{L}(6)\|/\|\tilde{L}(12)\| = 16$, correspond to the same value $a\Theta = 0.35$ rad, which means that most of the higher-order mode energy of the lift is contained in the first harmonic $n = 2$. For the swept blades, the minimum of $D = 5.5\%$ and the maximum of the ratio $\|\tilde{L}(6)\|/\|\tilde{L}(12)\| = 18.8$, also correspond to the same value $a\Theta = 0.35$ rad. Thus, it is possible to adjust the angle Θ of the trapezoidal obstructions or the Gaussian width parameter a so that $a\Theta = 0.35$ rad.

A value of $a\Theta = 0.1$ rad is chosen to illustrate the influence of the trapezoidal obstructions on the circumferential unsteady lift spectrum. In Fig. 9, v_0 and $v_m(R)$ were, respectively, set to 0 and -1 in Eqs. (14)

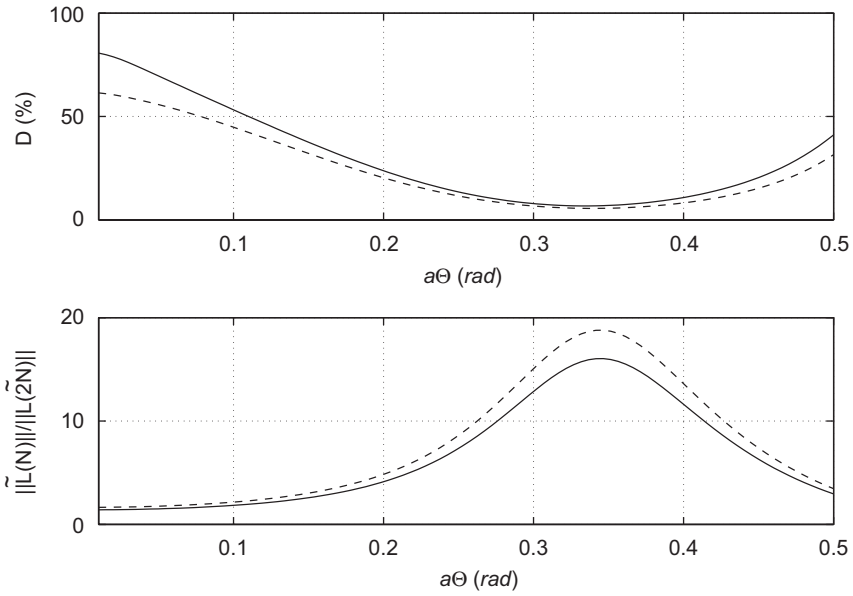

Fig. 8. Harmonic content indicators as a function of the product $a\Theta$, $R_1 = 8$, $R_2 = 12$ cm. Top: harmonic content rate D (%), bottom: ratio between the fundamental unsteady lift order and its first harmonic $\|\tilde{L}(N)\|/\|\tilde{L}(2N)\|$. Line: trapezoidal blades, dashed line: swept blades of an actual automotive fan.

and (19). The corresponding spatial velocity defect and the spatial unsteady lift $L(\theta)$ are shown in Fig. 9a and b. The Gaussian wake assumption is particularly well adapted to this small values of $a\Theta$ (similar to the wake measured by Staiger [28]). In Fig. 9b, the continuous line corresponds to the 35° trapezoidal blades and the dashed lines correspond to the automotive swept blades.

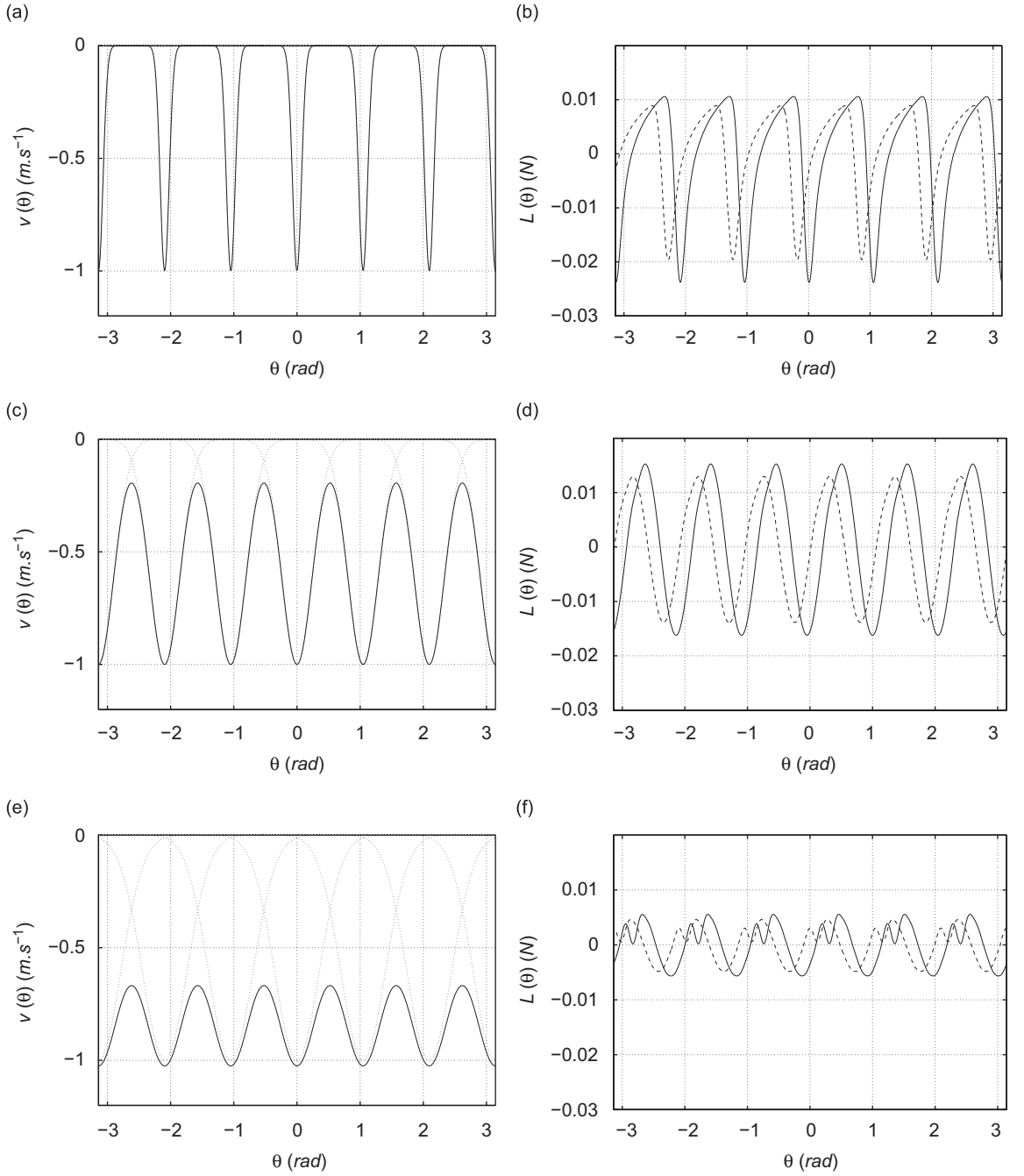

Fig. 9. Gaussian overlapping for different wake widths $a\Theta$. Left: velocity profile (dotted lines: individual Gaussian velocity profiles and continuous lines: sum of the individual velocity profiles): (a) $a\Theta = 0.1$, (c) $a\Theta = 0.35$, (e) $a\Theta = 0.5$. Right: spatial unsteady lift (continuous line: trapezoidal blades, dashed line: swept blades): (b) $a\Theta = 0.1$, (d) $a\Theta = 0.35$, (f) $a\Theta = 0.5$.

The imposed wake velocity profile generated when choosing the optimal product $a\Theta = 0.35$ rad is plotted in Fig. 9c, where the dotted lines correspond to individual Gaussian velocity profiles $e^{-((\theta-n\theta_0)/a(R)\Theta(R))^2}$ (generated by individual obstructions) and the continuous line corresponds to the sum of the individual velocity profiles $\sum_{n=-\infty}^{+\infty} e^{-((\theta-n\theta_0)/a(R)\Theta(R))^2}$ defined in Eq. (14). Low overlapping of the Gaussian wakes is observed for the optimal value $a\Theta = 0.35$ rad. The spatial unsteady lift due to this imposed wake velocity profile is plotted in Fig. 9d. It is clear that the lift fluctuation is almost sinusoidal.

The Gaussian overlapping at the large value $a\Theta = 0.5$ rad causes a strong velocity defect all around the circumference, as shown in Fig. 9e, and the Gaussian wake approximation may not longer be valid. The corresponding spatial unsteady lift shown in Fig. 9f.

In all cases, the magnitude of the unsteady lift is slightly larger for the trapezoidal blades and angular shift is also observed between the trapezoidal and the swept blades. Indeed, in practice, the blades are swept to reduce the unsteady lift by changing the phase along the leading edge when the encountered gust is radial (as it is the case for many stators and the trapezoidal obstructions).

Fig. 10 shows the normalized unsteady lift spectrum ($\tilde{L}(w = 6n)/\tilde{L}(6)$, $1 \leqslant n \leqslant 7$) associated to the optimal wake width $a\Theta = 0.35$ rad, and to the values $a\Theta = 0.1$, and $a\Theta = 0.5$ rad. As observed in Figs. 8 and 9, the harmonics of the fundamental circumferential order ($w = N = 6$) are more energetic in the case of $a\Theta = 0.1$ rad, or $a\Theta = 0.5$ rad than in the case of $a\Theta = 0.35$ rad, for $w \leqslant 42$, or $n \leqslant 7$. The harmonic content rates are $D_{a\Theta=0.5} = 21.7\%$, $D_{a\Theta=0.35} = 5.5\%$, and $D_{a\Theta=0.1} = 29.1\%$. Consequently, localized and deep velocity fluctuations correspond to the generation of many circumferential components in the lift spectrum. Therefore, sharp obstructions ($a\Theta = 0.1$ rad) or sharp circumferential zones between obstructions ($a\Theta = 0.5$ rad) are not appropriate to selectively control a circumferential mode of the lift. The ideal analytical case $a\Theta = 0.35$ rad ($D = 5.5\%$) will be considered as the low limit of the harmonic content rate in this paper.

Numerical parametrization of effects of the wake width generated by the rotor on the unsteady stator loading has been investigated by Waitz et al. [6] in turbomachines. They concluded that the Gaussian wake width at the inlet plane of the stator must be approximatively equal to the rotor pitch to maximize the amplitude of the BPF with respect to its harmonics (a $\frac{16}{40}$ rotor-stator pitch ratio was under investigation in Ref. [6]). In the present paper, the results of the optimization of the wake width $a\Theta$ generated by the trapezoidal obstruction lead to a wake width at mid-height of the velocity defect ($2a\Theta \ln 2 = 28^\circ$, as indicated in Fig. 5), which is a little smaller than the angle of the trapezoidal blades (35°). At the height v_m/e of the velocity defect, the wake width is $2a\Theta = 40^\circ$ (Fig. 5), which is a little larger than the angle of the trapezoidal blades (35°). Thus, the conclusion of Waitz et al. can also be applied to the case of stator (control obstruction) wakes impinging in rotor blades.

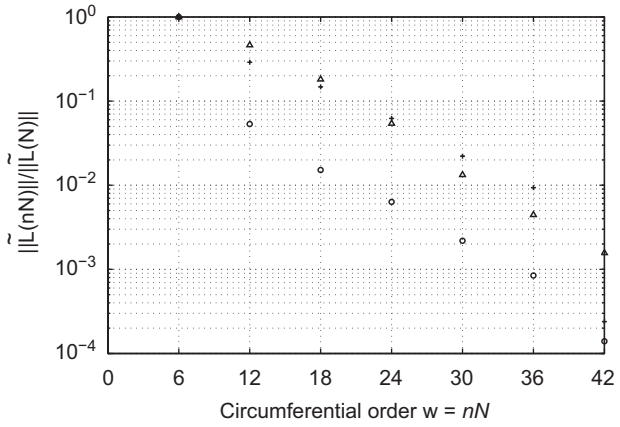

Fig. 10. Unsteady lift spectrum—rotor/6-trapezoidal obstructions interaction for different wake widths $a\Theta$: △, $a\Theta = 0.1$; o, $a\Theta = 0.35$; +, $a\Theta = 0.5$.

4.2. 6-periods sinusoidal obstruction

The mean wake velocity defect generated by the sinusoidal obstruction of Fig. 7b has been measured with a single hot wire anemometer. The velocity measurements have then been used to approximate the coefficients of the Gaussian function describing the velocity profile behind the obstruction. The hot wire was located at various radial positions between the sinusoidal obstruction (in the upstream flow) and the rotor, near the blade leading edges (0.5 cm). The hot wire anemometer was fixed and the sinusoidal obstruction was rotated from $-\pi/6$ to $\pi/6$ (an angular period) by increments of 2°. The hot wire signal was acquired for 3.4 s, corresponding to 159 revolutions of the fan rotating at 2800 rev min^{-1}. The sampling frequency was set to 4800 Hz to give 102 samples per revolution. The hot wire was aligned so that the voltage was maximum, which corresponds to a wire perpendicular to the blade leading edge, thus, giving an estimation of the transversal gust velocity (relative to the blade) generated by the sinusoidal obstruction.

Fig. 11 shows the measured mean velocity and the adjusted Gaussian approximation of the mean velocity at different radii, defined by Eq. (14). Moreover, the following Gaussian function is also assumed for the radial dependence of the inflow velocity magnitude:

$$v_m(R) = v_m e^{-((2R-R_1-R_2)/a_R(R_2-R_1))^2} \tag{24}$$

The best agreement between measured experimental data and the Gaussian approximation has been obtained for $a = 0.36$, $a_R = 0.5$, and $v_m = 2\,\mathrm{m\,s^{-1}}$. For simplicity, the circumferential width parameter a has been assumed independent of the radial position R. The coefficient $v_m(R)$ of the approximated Gaussian velocity function can then be introduced into Eq. (19). The angular sector $\Theta(R)$ of the sinusoidal obstruction as a function of the radius R defined in Eq. (22), and the parameter $a = 0.36$, are introduced in Eq. (15). Table 1 shows the ratio $\|\check{L}(N)\|/\|\check{L}(nN)\|$ ($N = 6$, $1<n<7$) of the rotor unsteady lift spectrum generated by the interaction between the sinusoidal obstruction and the rotor. The harmonics of the fundamental circumferential unsteady lift order $w = 6$ are significantly below the fundamental in the lift spectrum, leading to a relatively small harmonic content rate $D = 18.1\%$. In Ref. [1], these ratios are indirectly estimated through acoustical measurements up to the order $n = 4$ ($w = 24$). The sinusoidal obstruction therefore allows to control a circumferential order of the rotor unsteady lift without too much affecting the higher harmonics.

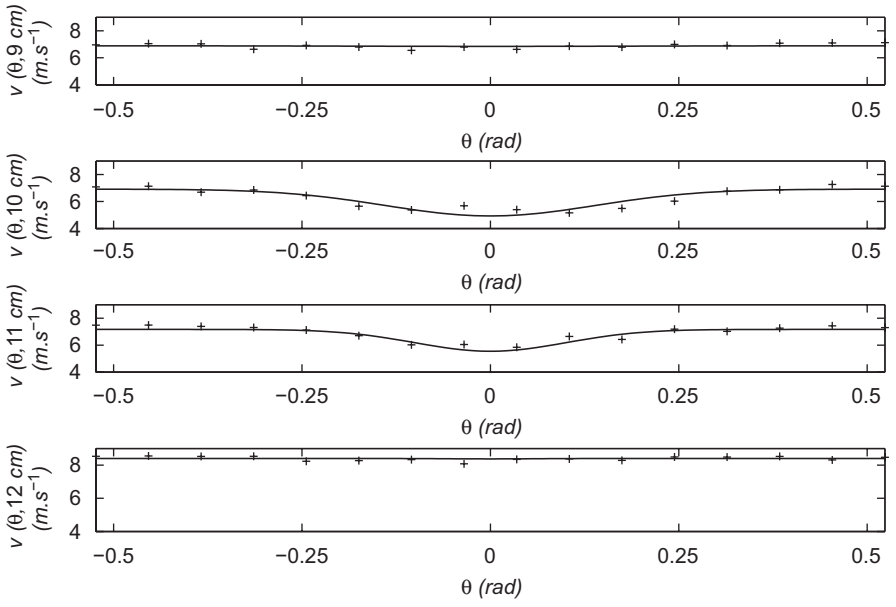

Fig. 11. Gaussian distribution approximation (line) of the measured mean velocity defect (crosses) in the case of the sinusoidal obstruction.

Table 1
$\|\tilde{L}(N)\|/\|\tilde{L}(nN)\|$ ratio as a function of nN for the sinusoidal obstruction

nN	6	12	18	24	30	36	42
$\|\tilde{L}(N)\|/\|\tilde{L}(nN)\|$	1	5.3	39.6	342	7.1×10^3	10.5×10^3	15.5×10^3

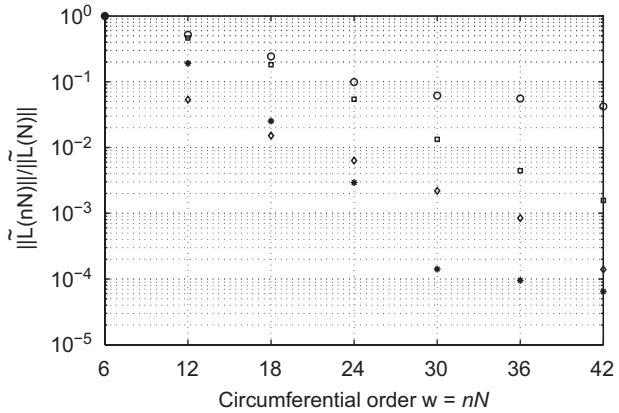

Fig. 12. Comparison of the predicted unsteady lift spectra generated by the rectangular (o), sinusoidal ($\star$) and trapezoidal obstructions ($\diamond$, $a\Theta = 0.35$; $\square$, $a\Theta = 0.1$) ($N = 6$).

In the next section, it is shown that the choice of narrow rectangular obstruction generates salient wakes, leading to a broader lift spectrum.

4.3. Six small-width rectangular obstructions

The main disadvantage of choosing small-width obstructions is that the wakes generated by the obstructions are very salient, leading to a high harmonic content rate of the unsteady lift.

This can lead to amplification of higher acoustic tones when controlling only the BPF as noted by Polacsek et al. [2] using rods: for a sound pressure level attenuation of 8 dB at the BPF, amplifications of 6, 15 and 11 dB were observed at the first, second and third harmonics of the BPF. The results presented by Neuhaus et al. [31] also show that the use of cylinders leads to an increase of the upper harmonics while controlling the BPF. The three-dimensional shape of cylinder is not included in the proposed model, i.e. the imposed Gaussian velocity behind cylindrical obstructions of diameter d would be the same as the Gaussian velocity imposed behind rectangular obstructions of width d.

A rectangular obstructions/rotor configuration using the 6-bladed rotor presented in this study and six rectangular obstructions of 14 mm in width is studied. The circumferential unsteady lift spectrum that it generates is compared to the spectra already shown in this paper for other obstruction shapes. The circumferential Gaussian width parameter a is set to 0.5. Moreover, no variation of the velocity profile is imposed along the radial direction ($a_R \to \infty$), similar to the simulations carried out in Sections 4.1 for the trapezoidal obstruction. In Fig. 12, the predicted unsteady lift spectrum generated by the rectangular obstructions/rotor configuration is compared to the unsteady lift spectrum generated by the 6-trapezoidal obstructions/rotor configurations ($a\Theta = 0.35$, 0.1 rad) and to the 6-sinusoidal obstruction/rotor interaction.

The unsteady lift spectra due to the rotor/rectangular obstructions interaction lead to a large harmonic content rate ($D = 58.6\%$). The salient wakes generated by the small rectangular obstructions lead to a broad lift spectrum. Thus, this solution is not selective and cannot be used to control only one mode without affecting the other modes. To be selective, larger obstructions (in the circumferential direction) must be chosen.

5. Conclusions

A simple analytical formulation has been derived to predict the unsteady lift generated by the interaction between a rotor and an obstruction, designed to control an acoustic tone generated by the rotor. For acoustically compact fans, an acoustic tone corresponding to a multiple of the BPF is associated with essentially a given circumferential mode of the blade unsteady lift; therefore, it is sufficient to control only this most radiating unsteady lift mode to control each acoustic tone. The principle of the control is thus to add a secondary unsteady lift mode, of equal intensity but opposite in phase with the primary unsteady lift mode so that the resultant of both primary and secondary lift modes is null. To control one unsteady lift mode (consequently an acoustic tone) without increasing the harmonics of the controlled mode (consequently the harmonics of the acoustic tone to be controlled), it is important for the secondary unsteady lift to be harmonically selective. The analytical formulation derived in this paper therefore provides a tool to simply evaluate the ability of the control obstruction to control one tone without affecting the other tones. The harmonic content rate of the unsteady lift generated by the proposed control obstructions can also be optimized with the proposed model.

The numerical examples show that physically compact obstructions generate salient wakes and therefore broad circumferential lift spectra. In such a case, controlling one lift mode can generate other undesirable modes. However, better designed control obstructions, such as optimized trapezoidal obstructions or sinusoidal obstructions, have a relatively low harmonic content rate. In Ref. [1], the unsteady lift spectrum and the harmonic content rate generated by the control obstructions are indirectly estimated from experimental acoustic pressure measurement.

To optimize the geometry of a control obstruction, the rotor blade geometry must be known. Then, assuming that the wake generated by the obstruction is Gaussian, the geometrical characteristics of the obstruction can be optimized. Conversely, geometry of rotor blades (mainly the chord and the sweep as a function of the radius) can be optimized by imposing a control obstruction geometry.

Further optimization of the obstruction/blade geometries could include some of the effects neglected in this paper. A second-order analysis could be investigated to take the blade camber and the mean flow angle of incidence into account [14]. Moreover, the developments of Filotas [11] or Mugridge [12] could be used to take into account non-transversal velocity profiles (e.g. derived from experimental or numerical prediction). Computational fluid dynamics (CFD) approaches could be used to refine the estimation of the pressure distribution on complex geometry blades, as proposed by Lu [17] or Maaloum [20]. CFD can also be useful to evaluate the non-stationary part of the flow.

Acknowledgments

This work has been supported by the AUTO21 Network of Centres of Excellence (Canada) and Siemens VDO Automotive Inc. The authors wish to thank Sylvain Nadeau formerly from Siemens Automotive Inc. and Jacky Tartarin from the Université de Poitiers (France) for their collaboration to this research.

References

[1] A. Gérard, A. Berry, P. Masson, Y. Gervais, Experimental validation of tonal noise control from subsonic axial fans using flow control obstructions, *Journal of Sound and Vibration* (2008), in press, doi:10.1016/j.jsv.2008.09.019.

[2] C. Polacsek, F. Desbois-Lavergne, Fan interaction noise reduction using a wake generator: experiments and computational aeroacoustics, *Journal of Sound and Vibration* 265 (4) (2003) 725–743.

[3] P.A. Nelson, Active techniques and their potential for application in aeroacoustics, Keynote lecture, *6th AIAA/CEAS Aeroacoustic Conference*, Lahaina, Hawaï, 2000.

[4] K.J. Farrell, S.G. Walter, Technique for reducing acoustic radiation in turbomachinery, Patent No. US 6,375,416, April 23, 2002.

[5] A.O. Andersson, Active control of tone noise in engine ducts, Patent No. PCT/US95/09999 (WO 96/03585), February 8, 1996.

[6] I.A. Waitz, J.M. Brookfield, J. Sell, B.J. Hayden, Preliminary assessment of wake management strategies for reduction of turbomachinery fan noise, *Journal of Propulsion and Power* 12 (5) (1996) 958–966.

[7] T. Theodorsen, General theory of aerodynamic instability and the mechanism of flutter, NACA Technical Report 435, 1935.

[8] W.R. Sears, Some aspects of non-stationary airfoil theory and its practical application, *Journal of the Aeronautical Sciences* 8 (3) (1941) 104–108.
[9] T.V. Kármán, W.R. Sears, Airfoil theory for non-uniform motion, *Journal of the Aeronautical Sciences* 5 (10) (1938) 379–390.
[10] J.H. Horlock, Fluctuating lift forces on aerofoils moving through transverse and chordwise gusts, *Journal of Basic Engineering, Transactions of the ASME* 90 (1968) 494–500.
[11] L.T. Filotas, Theory of airfoil response in a gusty atmosphere. Part 1: aerodynamic transfer function, Institute of Aeronautics and Space, University of Toronto, UTIAS, Report 139, 1969.
[12] B.D. Mugridge, Gust loading on a thin aerofoil, *The Aeronautical Quarterly* 22 (3) (1971) 301–310.
[13] R.K. Amiet, Compressibility effects in unsteady thin-airfoil theory, *AIAA Journal* 12 (1974) 252–255.
[14] H.M. Atassi, The Sears problem for a lifting airfoil revisited—new results, *Journal of Fluid Mechanics* 141 (1984) 109–122.
[16] N. Namba, Three-dimensional analysis of blade force and sound generation for an annular cascade in distorted flows, *Journal of Sound and Vibration* 50 (4) (1977) 479–508.
[17] H.Z. Lu, L. Huang, R.M.C. So, J. Wang, A computational study of the interaction noise from a small axial-flow fan, *Journal of the Acoustical Society of America* 122 (3) (2007) 1404–1415.
[18] S. Timouchev, A. Nedashkovsky, G. Pavic, Experimental validation of axial fan 3D acoustic-vortex method CFD-CAA study, Fan Noise 2007, Lyon, France, 2007.
[19] H. Reese, T. Carolus, C. Kato, Numerical prediction of the aeroacoustic sound sources in a low pressure axial fan with inflow distortion, Fan Noise 2007, Lyon, France, 2007.
[20] A. Maaloum, S. Kouidri, R. Rey, Aeroacoustic performance evaluation of axial flow fans based on the unsteady pressure field on the blade surface, *Applied Acoustics* 65 (2004) 367–384.
[22] M.E. Goldstein, *Aeroacoustics*, McGraw-Hill Inc., New York, USA, 1976.
[23] W.K. Blake, *Mechanics of Flow-induced Sound and Vibration. Vol. 2: Complex Flow Structure Interaction*, Academic Press Inc., London, 1986 (Chapter 12.4).
[25] M.V. Lowson, Theoretical analysis of compressor noise, *Journal of the Acoustical Society of America* 47 (1) (1968) 371–385.
[26] G. Krishnappa, Blade interaction noise from lift fans, *Journal of the Acoustical Society of America* 51 (1) (1971) 1464–1470.
[27] S. Subramanian, T.J. Mueller, An experimental study of propeller noise due to cyclic flow distortion, *Journal of Sound and Vibration* 183 (5) (1995) 907–923.
[28] M. Staiger, H. Stetter, Periodic aerodynamic response of axial fan rotor blades to non-uniform inlet flow fields, *International Gas Turbine and Aeroengine Congress and Exhibition*, Birmingham, UK, 1996.
[29] S.C. Morris, J.J. Good, J.F. Foss, Velocity measurements in the wake of an automotive cooling fan, *Experimental Thermal and Fluid Science* 17 (1998) 100–106.
[30] M.R. Spiegel, *Mathematical Handbook of Formulas and Tables*, McGraw-Hill Book Company, New York, 1968.
[31] L. Neuhaus, J. Schulz, W. Neise, M. Möser, Active control of the aerodynamic performance and tonal noise of axial turbomachines, *Proceedings Institution of Mechanical Engineers* 217 (2003) 375–383.
[32] V. Kota, M.C.M. Wright, Wake generator control of inlet flow to cancel flow distortion noise, *Journal of Sound and Vibration* 295 (2006) 94–113.